Evaluating the Recent "2+26" Regional Strategy for Air Quality Improvement During Two Orange Air Pollution Alerts in Beijing: variations of PM$_{2.5}$ concentrations, source apportionment, and the relative contribution of local emission and regional transport

Ziyue Chen[1,2], Danlu Chen[1], Nianliang Cheng[3,4], Yan Zhuang[1], Mei-Po Kwan[5,6], Bin Chen[7], Bo Zhao[8], Lin Yang[9*], Bingbo Gao[10], Ruiyuan Li[1], Bing Xu[11*]

[1] State Key Laboratory of Earth Surface Processes and Resource Ecology, College of Global and Earth System Sciences, Beijing Normal University,19 Xinjiekou Street, Haidian, Beijing 100875, China

[2] Joint Center for Global Change Studies, Beijing 100875, China

[3] Chinese Research Academy of Environmental Sciences, Beijing 100012, China

[4] Beijing Municipal Environmental Monitoring Center, Beijing 100048, China

[5] Department of Geography and Geographic Information Science, University of Illinois at Urbana-Champaign, Urbana, IL 61801, USA

[6] Department of Human Geography and Spatial Planning, Utrecht University, 3584 CB Utrecht, The Netherlands

[7] Department of Land, Air and Water Resources, University of California, Davis, CA 95616, USA

[8] College of Earth, Ocean, and Atmospheric Sciences, Oregon State University, Oregon, USA

[9] School of Geographic and Oceanographic Sciences, Nanjing University, Nanjing,210023, China

[10] National Engineering Research Center for Information Technology in Agricultre,11 Shuguang Hua yuan Middle Road, Beijing 100097, China

[11] Ministry of Education Key Laboratory for Earth System Modeling, Department of Earth System Science, Tsinghua University, Beijing 100084, China

*To whom correspondence should be addressed. Email: yanglin@nju.edu.cn or bingxu@tsinghua.edu.cn

Abstract

To comprehensively evaluate the effects of the recent "2+26" regional strategy for air quality improvement, we compared the variations in PM$_{2.5}$ concentrations in Beijing during four pollution episodes with different emission-reduction strategies. The "2+26" strategy implemented in March 2018 led to a mean PM$_{2.5}$ concentrations of 16.43% lower than that during the pollution episode in March 2013, when no specific emission-reduction measures were in place. The same "2+26" strategy implemented in November 2017 led to a mean PM$_{2.5}$ concentrations of 32.70% lower than that during the pollution episode in November 2016, when local emission-reduction measures were implemented. The results suggested that the effects of the "2+26" regional emission-reduction measures on PM$_{2.5}$ reductions were influenced by a diversity of factors and could differ significantly during specific pollution episodes. Furthermore, we found the

Atmospheric
Chemistry
and Physics
Discussions

37   proportions of sulfate ions decreased significantly and nitrate ions were the dominant $PM_{2.5}$

38   components during the two "2+26" orange alert periods. Meanwhile, the relative contributions of

39   coal combustion to $PM_{2.5}$ concentrations in Beijing during the pollution episodes in March 2013,

40   November 2016, November 2017 and March 2018 was 40%, 34%, 28% and 11% respectively,

41   indicating that the recent "Coal to Gas" project and the contingent "2+26" strategy led to a

42   dramatic decrease in coal combustion in the Beijing-Tianjin-Hebei Region. On the other hand, the

43   relative contribution of vehicle exhaust during the "2+26" orange alert periods in November 2017

44   and March 2018 reached 40% and 54% respectively. The relative contribution of local emission to

45   $PM_{2.5}$ concentrations in Beijing also varied significantly and ranged from 49.46% to 89.35%

46   during the four pollution episodes. These results suggested that the "2+26" regional

47   emission-reduction strategy should be implemented with red air pollution alerts during heavy

48   pollution episodes to intendedly reduce the dominant contribution of vehicle exhausts to $PM_{2.5}$

49   concentrations in Beijing, while specific emission-reduction measures should be implemented

50   accordingly for different cities within the "2+26" framework.

51   **Keywords**: **Air pollution alert; Regional integration; Emission reduction;**

52   **WRF-CAMx; Beijing; "2+26".**

53   ## 1 Introduction

54   In January 2013, a severe haze episode with the highest concentration of hourly fine particulate

55   matter with a diameter of less than 2.5 micrometers ($PM_{2.5}$) occurred in Beijing (886 μg/ m^3),

56   which attracted worldwide attention. Since 2013, Beijing, located in the Beijing-Tianjin-Hebei

57   region, has been a heavily polluted area in China that suffers from continuous haze episodes

58   associated with high concentrations of $PM_{2.5}$, especially in winter. Given the significant negative

59   influence of $PM_{2.5}$ on public health (Garrett and Casimiro, 2011; Guaita et al., 2011; Pasca et al.,

60   2014; Li et al., 2015), the air quality management authority in Beijing has put growing emphasis

61   on long-term environmental protection policies, including shutting down polluting factories and

62   limiting vehicle use through license plate rules. However, total emissions of airborne pollutants

63   remain at very high levels in Beijing, leading to frequent heavy pollution episodes (Guo et al.,

64   2012). To mitigate this problem, contingent emission-reduction measures, in addition to regular

65   environmental policies, are necessary in Beijing in order to improve local air quality during air

66   pollution episodes.

67   In 2013, the Beijing Municipal Government published the "Heavy Air Pollution Contingency

68   Plan" and revised this plan in 2015 to better manage air quality during pollution episodes.

69   According to the predicted concentrations of different airborne pollutants and the duration of

70   pollution episodes, there are four levels of air pollution alerts for Beijing, which are blue, yellow,

71   orange, and red alerts. Specific emission-reduction measures are implemented when each type of

72   air pollution alerts is in effect. The red alert is the most stringent level of air pollution alerts and

73   predicts severe air pollution episodes (Air Quality Index [AQI] >300) that will last for more than

74   three days. Emission-reduction measures during red alerts mainly include the implementation of

75   the odd-even license plate policy (only about half of all of the cars in Beijing is allowed to run

76   within the fifth-ring district in each day), the suspension of all outdoor construction work and
77   temporary shutdown of listed polluting factories. The orange alert predicts heavy air pollution
78   episodes (AQI >200) that will last for more than three days. Emission-reduction measures during
79   orange alerts mainly include forbidding vehicles that cannot meet the Environmental Standard
80   Levels I and II, the suspension of specific outdoor work (e.g., painting) and temporary shutdown
81   of listed polluting factories (the list for red alerts includes more factories than that for orange
82   alerts). The blue and yellow alerts predict heavy air pollution episodes that will last for more than
83   one and two days respectively. There are very few compulsory emission-reduction measures for
84   blue and yellow alerts and most emission-reduction measures are suggestive. The characteristics
85   and effects of these emission-reduction measures during alert periods have been massively studied
86   (Zhong, J. et al., 2017; Zhang, Z. et al.,2017; Wang, X. et al., 2017; Zeng, W. et al., 2018; Shang,
87   X. et al., 2018). However, previous emission-reduction measures during orange and red alerts
88   were solely conducted in a specific city (e.g., Beijing) while regional emission-reduction measures
89   implemented simultaneously in many adjacent cities have rarely been implemented and evaluated.

90   Although the peak $PM_{2.5}$ concentrations in Beijing could be reduced by 20% through strict
91   emission-reduction measures (Cheng et al., 2017), local $PM_{2.5}$ concentrations remained at very
92   high levels during red alert periods. This is mainly attributed to the regional transport of airborne
93   pollutants from neighboring cities to Beijing (Chen et al., 2016). Therefore, regional integration
94   has become one of the major solutions for further reducing $PM_{2.5}$ concentrations in Beijing during
95   heavy pollution episodes. To promote this strategy, the Ministry of Environmental Protection of
96   the People's Republic of China released the "2017 Air Pollution Prevention and Management Plan
97   for the Beijing-Tianjin-Hebei Region and its Surrounding Areas" (MEP, 2017). This plan suggests
98   that Beijing, Tianjin, eight cities in Hebei Province, four cities in Shanxi Province, seven cities in
99   Shandong Province and seven cities in Henan Province (2+26) constitute the regional network
100 involved in the long-distance transport of airborne pollutants surrounding Beijing. Therefore,
101 during heavy pollution episodes, unified emission-reduction measures should be carried out in
102 these cities simultaneously to reduce extremely high $PM_{2.5}$ concentrations in Beijing.

103 Since the launch of the "2+26" plan, Beijing experienced two pollution episodes in November
104 2017 and March 2018, when MEP released two orange alerts and implemented corresponding
105 emission-reduction measures in all 28 cities simultaneously. The two orange alerts were the first
106 two attempts of the "2+26" plan to reduce $PM_{2.5}$ concentrations in Beijing. To better evaluate this
107 "2+26" regional strategy and for a comprehensive comparison, we also included in this study two
108 other pollution episodes in Beijing: November 2016 (with local emission-reduction measures) and
109 March 2013 (with no emission-reduction measure). We first analyzed the variations in $PM_{2.5}$
110 concentrations in Beijing during the four pollution episodes. Following this, we quantified the
111 component and sources of the $PM_{2.5}$. Based on source apportionment, we further quantified the
112 relative contributions of local emissions and regional transport to $PM_{2.5}$ concentrations in Beijing
113 during these four pollution episodes. The methodology and findings of this research not only holds
114 practical significance for further improving the "2+26" regional strategy, but also shed some light
115 on the regional integration of air quality management in other parts of China.

Atmospheric
Chemistry
and Physics
Discussions

2 Materials and methods

2.1 Study sites

Beijing is located at the northwestern edge of the North China Plain. It is surrounded by mountains on three sides, resulting in a geographical condition unfavorable for the dispersion of airborne pollutants. Therefore, air pollution episodes have been frequently witnessed in Beijing since 2013, especially in winter. Based on large-scale field-experiments and model simulation, MEP (2017) pointed out that 28 cities formed a regional transport network of airborne pollutants, which influenced local $PM_{2.5}$ concentrations in Beijing significantly. These 28 cities include two municipalities directly under the central government, Beijing and Tianjin and another 26 neighboring cities surrounding Beijing, which are Shijiazhuang, Tangshan, Lang fang, Baoding, Cangzhou, Hengshui, Xingtai and Handan in Hebei Province, Taiyuan, Yangquan, Changzhi and Jincheng in Shanxi Province, Jinan, Zibo, Jining, Dezhou, Liaocheng, Binzhou and Heze in Shandong Province, Zhengzhou, Kaifeng, Anyang, Hebi, Xinxiang, Jiaozuo and Puyang in Henan Province. The locations of these cities are shown in Fig 1. These 26 cities, especially those cities located in the Hebei provinces, are mainly industrial cities that consume a large amount of coals and produce massive amounts of airborne pollutants. To comprehensively understand the effects of the "2+26" regional strategy for air quality improvement in Beijing, all these 28 cities were selected as study sites for this research.
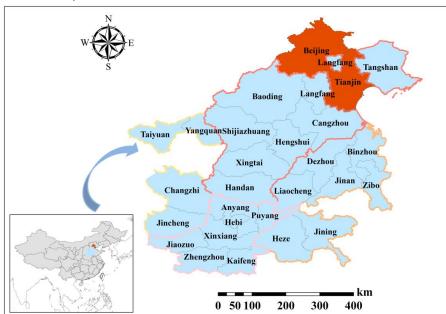

Fig 1. Geographical locations of the 28 cities within the "2+26" regional integration framework

Atmospheric
Chemistry
and Physics
Discussions

2.2 Data Sources

2.2.1 Ground PM$_{2.5}$ and meteorological observation data

137 The data of major airborne pollutants for this research were collected from the website PM25.in.
138 This website assembles official data of major airborne pollutants provided by the China National
139 Environmental Monitoring Center (CNEMC) and publishes hourly air quality information for 367
140 monitored cities in China, which include all of the 28 cities in the "2+26" framework. By using a
141 specific API (Application Programming Interface) provided by PM25.in, we collected hourly
142 pollutant data (e.g., PM$_{2.5}$, CO, NO$_2$, O$_3$) for these 28 cities. The hourly average concentration of
143 each pollutant for one city is calculated by averaging the hourly value measured at all available
144 observation stations within the city. For the following analysis, we employed time series air
145 quality data covering all four pollution periods: from 0 AM, November 24th to 12 PM, November
146 27th, 2016; from 0 AM, November 4th, 2017 to 12 PM, November 7th, 2017; from 0 AM, March
147 14th to 12 PM, March 17th, 2013; from 0 AM March 11th to 12 PM, March 14th, 2018.

150 In addition to large-scale meteorological data for the following simulation, we also employed
151 ground observation data to compare meteorological conditions during these four pollution
152 episodes. Meteorological data for this research were collected at the Guanxiangtai Station in
153 Beijing and were downloaded from the Department of Atmospheric Science of the University of
154 Wyoming (http://weather.uwyo.edu/upperair/sounding.html). Based on the comparison of the
155 meteorological data, we could ascertain whether large variations in meteorological conditions
156 existed between the four pollution episodes, as a potential influencing factor of the variations in
157 PM$_{2.5}$ concentrations.

2.2.2 PM$_{2.5}$ component Data

159 To comprehensively understand the component of PM$_{2.5}$ during the four pollution episodes, we
160 collected PM$_{2.5}$ sample data at the DongSi Station for further analysis. These PM$_{2.5}$ sample data
161 were collected during the pollution episodes in March, 2013, November 2016, November 2017
162 and March 2018 respectively. We employed an URG-9000B Ambient Ion monitor (Thermo Fisher
163 Scientific), which includes two Dionex ICS-90 ion chromatography systems (DIONEX, US), to
164 detect water soluble ion Na$^+$, Mg^{2+}, Ca^{2+}、K$^+$、NH$_4$$^+$、Cl$^-$、SO$_4$$^{2-}$、NO$_3$$^-$、PO$_4$$^{3-}$. The original temporal
165 resolution for ion detection was 15 minutes and for the comparison with other components, the
166 resolution for water-soluble ion detection was averaged to an hour. The organic carbon
167 concentration of PM$_{2.5}$ was analyzed using the OC/EC organic carbon analyzer (sunset lab model
168 5l) and the temporal resolution for carbon detection was an hour. The in-depth analysis of PM$_{2.5}$
169 component provides significant reference for understanding the evolution and sources of PM$_{2.5}$
170 during the pollution episodes.

2.3 Method

2.3.1 Simulation Models

173 We employed the WRF-CAMx model for simulating the effects of emission reduction measures
174 on the reduction of major airborne pollutants. The WRF-CAMx includes three models: the

Atmospheric
Chemistry
and Physics
Discussions

175   middle-scale   meteorology   model   (WRF),   the   source   emission   model   (SMOKE)
176   (https://www.cmascenter.org/cmaq/) and air quality model (CAMx) (http://www.camx.com/). The
177   WRF model provided the meteorological field for the analysis. The CAMx model has been widely
178   used for simulating the evolution of air pollution episodes (An et al., 2007; Liu et al., 2010) and
179   was employed for simulating the variations of airborne pollutants in this study (ENVIRON, 2013).
180   In this research, the central point for the CAMx was set at the coordinate (35 °N, 110 °E) and
181   bi-directional nested technology was employed, producing two layers of grids with a horizontal
182   resolution of 36 km and 12 km respectively. The first layer of the grids has a 36km resolution and
183   200*160 cells covering most areas in East Asia (including Japan, South Korea, China, North
184   Korea, and other countries). The second layer of the grids has a 12km resolution and 120*102
185   cells, based on the lambert map projection and standard latitude lines 24 °N and 46 °N, covering the
186   North China Plain, which includes the Beijing-Tianjin-Hebei region, Shandong and Henan
187   Provinces. The vertical layer was divided into 20 unequal layers, eight of which were of
188   less-than-1km distance to the ground for better featuring of the structure of atmospheric boundary.
189   Airborne pollutants in CAMx were simulated according to some physical and chemical
190   mechanisms, including: a) horizontal advection scheme (PPM), b) implicit Euler vertical
191   convection scheme, c) the horizontal diffusion of K theory, d) Saprc99 gas-phase chemical
192   mechanism, and e) EBI calculation method. The initial and boundary conditions for simulating
193   airborne pollutants were set using the default CAMx profiles. For better simulating the pollution
194   process with longer time series, the simulation period was set as the entire March 2013, November
195   2016, November 2017, and March 2018. For the first running of this model, a spin-up period of 5
196   days was set to simulate the initial field and the following initial field was decided by the output of
197   previous simulations. Hence, the accumulation effects of emission sources have been
198   comprehensively considered and the influence of uncertain initial conditions has been reduced
199   significantly.

200   We employed ARW-WRF3.2 to simulate the meteorological field. The setting of the center and the
201   bi-directional nest for the WRF was similar to that of the CAMx as mentioned above. There were
202   35 vertical layers for the WRF and the outer layer provided boundary conditions of the inner layer.
203   The meteorological background field and boundary information with a GFS resolution of $1°×1°$
204   and temporal resolution of 6h were acquired from NCAR (National Center for Atmospheric
205   Research, https://ncar.ucar.edu/) and NCEP (National Centers for Environmental Prediction)
206   respectively. The terrain and underlying surface information was obtained from the USGS 30s
207   global DEM (https://earthquake.usgs.gov/). The output from the WRF model was interpolated to
208   the region and grid for the CAMx model using the Meteorology-Chemistry Interface Processor
209   (MCIP, https://www.cmascenter.org/mcip). The meteorological factors used for this model include
210   temperature, air pressure, humidity, geopotential height, zonal wind, meridional wind,
211   precipitation, boundary layer heights and so forth. An estimation model for terrestrial ecosystem
212   MEGAN (http://ab.inf.uni-tuebingen.de/software/megan/) was employed to process the natural
213   emissions. Anthropogenic emission data were from the Multi-resolution Emission Inventory for
214   China, MEIC $0.5°×0.5°$ emission inventory (http://www.meicmodel.org/) and Beijing emission
215   inventory (http://www.cee.cn/). We input the processed natural and anthropogenic emission data
216   into the SMOKE model and acquired comprehensive emission source files.

217

218 **Table 1 Sources of Emission inventory**

Airborne Pollutants	Sources	Data description
$PM_{2.5}$, BC, OC	MEIC	Resolution: 0.5 °×0.5 °
SO_2	Survey of Emission sources	Point sources, Polygon sources
NOx	Survey of Emission sources	Point sources, Polygon sources
PM_{10}	Survey of Emission sources	Point sources, Polygon sources
NH_3	MEIC	Resolution: 1 °×1 °
Anthropogenic VOCs	MEIC	Resolution: 0.5 °×0.5 °
Natural VOCs	MEGAN	Corresponding Grid data

219 **2.3.2 Source Apportionment**

220 PSAT (Particulate Matter Source Apportionment Technology) is one major extension of the
221 CAMx model. PSAT was developed from the related ozone source apportionment method and
222 provided PM source apportionment for specific geographic regions and source categories (Huang,
223 Q. et al.,2012). Furthermore, PSAT can be used to analyze the source-acceptor relationship of
224 $PM_{2.5}$ pollutants, and trace SO_2, SO_4^{2-}, NO_3^-, NH_4^+, SOA, Hg, EC, dust particles, and other
225 primary and secondary particles. As a species tagging method, PSAT tracks the regional source
226 and industry source of environmental receptor $PM_{2.5}$ and its main chemical components, and then
227 evaluates the contribution of initial conditions and boundary conditions to PM generation. By
228 identifying and tracking the transport, diffusion, transformation and decomposion of pollutants
229 emitted from various sources, PSAT estimates the relative contribution of different emission
230 sources to the spatial distribution of PM concentrations based on the analysis of mass balance.
231 PSAT-based source apportionment is conducted using reactive tracers that simulate the nonlinear
232 transformation between primary PM and secondary PM and are highly efficient and flexible for
233 source apportionment from the perspective of geographical source regions, emissions source
234 categories and individual sources (Burr, M. et al.,2011). PSAT effectively avoids the concentration
235 biases caused by Brute-force based source-closure methods that ignores non-linear chemical
236 processes and has been widely in previous studies (Xing, J. et al.,2011; Huang, Q. et al.,2012; Wu,
237 D. et al.,2013; Li, X. et al., 2015; Li, Y. et al., 2015). For this research, we established a regional
238 transport matrix between pollution sources and environmental receptors. According to the
239 provincial administrative division, the national grid is divided into 17 divisions, each of which
240 represents a provincial unit, and all other cells outside the national boundary are classified as Class
241 I, including the ocean and other areas. According to the scope of the Beijing-Tianjin-Hebei Region
242 and the "2+26" network, we further divide the study area into 13 sub-divisions, including Beijing,
243 Tianjin, eight cities in Hebei Province, Henan Province, Shandong Province and Shanxi Province,
244 for quantifying the influence of local emission and regional transport on the variations in $PM_{2.5}$
245 concentrations in Beijing during the four pollution episodes.

Atmospheric
Chemistry
and Physics
Discussions

2.4 Model verification

For the mean $PM_{2.5}$ concentrations in Beijing, we compared the observed and model estimated
$PM_{2.5}$ concentrations during the four pollution episodes to verify the accuracy of the WRF-CAMx
model (Fig 2). According to Fig 2, a general agreement was found between the simulated and
observed data with more than 85% of data points falling into the siege area of 1:2 and 2:1 lines.
WRF-CAMx slightly underestimated $PM_{2.5}$ concentrations due to the uncertainty in the emission
inventory, meteorological field simulation errors and insufficient chemical reaction mechanisms.
For the four pollution episodes, the correlation coefficient R, normalized mean bias (NMB),
normalized mean error (NME), mean fractional bias (MFB) and mean fractional error (MFE)
between observed and simulated data ranged from 0.65~0.80, -21%~-10%, 19%~32%, -31%~-8%,
and 12%~34% respectively, indicating a satisfactory simulation output (Boylan et al., 2006).
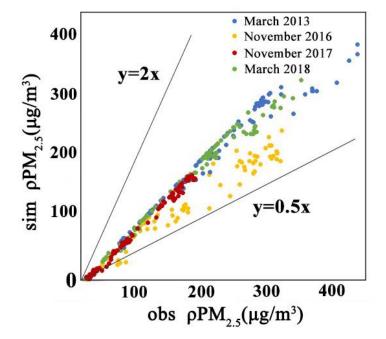

Fig 2. The comparison of observed and model simulated $PM_{2.5}$ concentrations in Beijing during four pollution episodes.

3 Results

3.1 Temporal variations in $PM_{2.5}$ concentrations during the four pollution episodes

Chen et al. (2017, 2018) suggested that wind speed and relative humidity were the major
meteorological factors that influenced wintertime $PM_{2.5}$ concentrations in Beijing. Based on the

Atmospheric
Chemistry
and Physics
Discussions

265   ground observation data, we found that the two meteorological factors during the pollution
266   episode in November 2016 was fairly similar to that during the orange alert period in November
267   2017, while the meteorological condition during the pollution episode in March 2013 was fairly
268   similar to that during the orange alert period in March 2018 (as shown in Table 2). According to
269   Table 2, all the four pollution episodes experienced a high-humidity and weak-wind condition.
270   Specifically, the fairly high relative humidity for the "2+26" orange alert period in November
271   2017 and the fairly low wind speed for the "2+26" orange alert period in March 2018 led to
272   extremely unfavorable conditions for the dispersion of airborne pollutants.

273   **Table 2 Major meteorological conditions during the four pollution episodes.**

Pollution Episodes	Mean Relative Humidity(%)	Mean Wind Speed(m/s)
March, 2013 (No emission-reduction)	56.25	2.32
March, 2018 ("2+26" strategy)	57.25	1.72
November, 2016 (Local emission-reduction)	58.25	2.37
November, 2017 ("2+26" strategy)	72.25	2.09

274   When the meteorological influences on the variations of $PM_{2.5}$ concentrations were limited, a
275   comparison between the $PM_{2.5}$ concentrations during these two orange alert periods and that
276   during the two corresponding pollution episodes provides useful reference for evaluating the
277   effects of "2+26" strategy on $PM_{2.5}$ reductions during the pollution episodes, which are usually
278   observed under a stagnant atmospheric condition, with high relative humidity and low wind speed.
279   The temporal variations in $PM_{2.5}$ concentrations during the two "2+26" orange alerts and the two
280   corresponding pollution episodes are shown in Table 3 and Fig 3.

281   **Table 3 Characteristics of $PM_{2.5}$ concentrations during four pollution episodes**

Pollution episode	Mean ($\mu g/m^3$)	Peak ($\mu g/m^3$)	Duration of $PM_{2.5}>100$ $\mu g/m^3$ (h)	Duration of $PM_{2.5}>150$ $\mu g/m^3$ (h)	Duration of $PM_{2.5}>200$ $\mu g/m^3$ (h)	Period with $PM_{2.5}>300$ $\mu g/m^3$ (h)
March, 2013 (No emission-reduction)	208.49	426.12	10	24	37	12
March, 2018 ("2+26" strategy)	174.24	325.91	6	10	44	5
November, 2016 (Local emission-reduction)	138.05	310.30	14	9	26	5
November, 2017 ("2+26" strategy)	92.91	176.20	24	24	0	0

282

Atmospheric
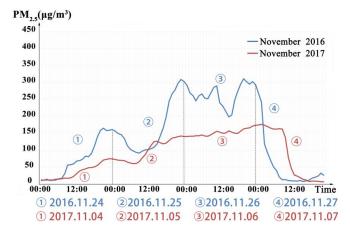Chemistry
and Physics
Discussions

Open Access

Fig 3. Variations of PM$_{2.5}$ concentrations during four pollution episodes with different emission-reduction measures in Beijing

As shown in Table 3 and Figure 3, both the peak and average PM$_{2.5}$ concentrations during the two orange alert periods were remarkably lower than those during the two corresponding pollution episodes with similar initial PM$_{2.5}$ levels and meteorological conditions. For the pollution episode in March 2013 and March 2018, PM$_{2.5}$ concentrations were both around 50μg/ m^3 at the beginning of both periods. Similarly, for the pollution episode in November 2016 and November 2017, the initial PM$_{2.5}$ concentrations were both around 15 μg/m^3 at the beginning of both periods. Following the similar initial PM$_{2.5}$ concentrations, it is noted that PM$_{2.5}$ concentrations increased at a much lower rate and further led to a lower peak and average PM$_{2.5}$ concentrations during the two orange alert periods.

According to Table 3, the mean and peak PM$_{2.5}$ concentrations during the "2+26" orange alert period in March, 2018 was 16.43% and 23.52% lower than those during the pollution episode in March 2018 respectively. Meanwhile, the duration with extremely high PM$_{2.5}$ concentrations was notably shorter during the orange alert period. The "2+26" strategy implemented during the

Atmospheric
Chemistry
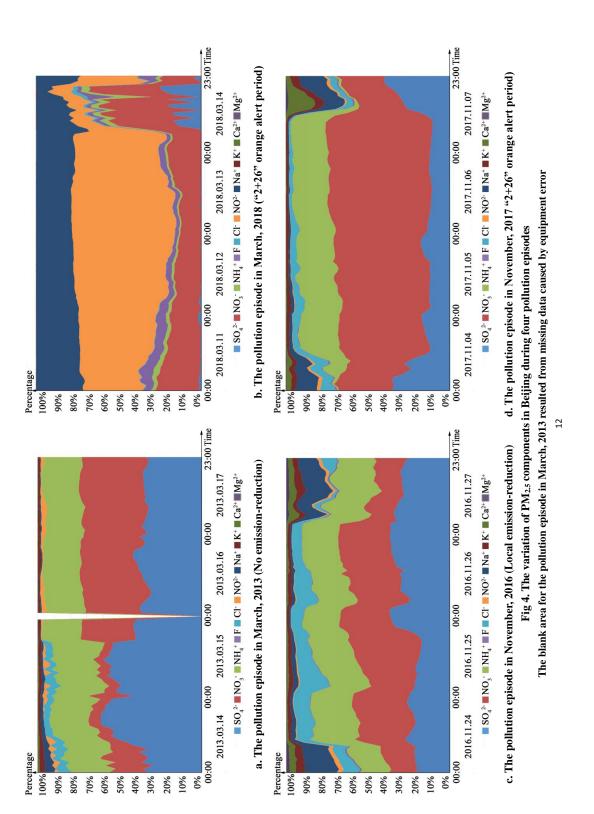and Physics
Discussions

298   orange alert period in November 2017 led to even better effects on $PM_{2.5}$ reductions. The mean

299   and peak $PM_{2.5}$ concentrations during this period was 32.70% and 43.22% lower than those during

300   the pollution episode in November 2016 respectively. More importantly, during the entire orange

301   alert period, $PM_{2.5}$ concentrations were constantly lower than 200 μg/m^3, indicating a highly

302   efficient control of high $PM_{2.5}$ concentrations.

303   **3.2 $PM_{2.5}$ component analysis during four pollution episodes**

304   The temporal variations of different $PM_{2.5}$ components during the four pollution episodes are

305   shown in Fig 4. As the figure indicates, the components of $PM_{2.5}$ in Beijing during the four

306   pollution episodes had notable variations.

a. The pollution episode in March, 2013 (No emission-reduction)

b. The pollution episode in March, 2018 ("2+26" orange alert period)

c. The pollution episode in November, 2016 (Local emission-reduction)

d. The pollution episode in November, 2017 "2+26" orange alert period)

Fig 4. The variation of PM$_{2.5}$ components in Beijing during four pollution episodes

The blank area for the pollution episode in March, 2013 resulted from missing data caused by equipment error

Atmospheric
Chemistry
and Physics
Discussions

307   For the four pollution episodes with different emission-reduction measures, the main components

308   for $PM_{2.5}$ were all SO_4^{2-}, NO_3^-, and NH_4^+. However, some major differences existed. With no or

309   only local emission-reduction measures implemented, the dominant $PM_{2.5}$ components was SO_4^{2-}

310   for the pollution episode in March 2013 and November 2016. During two "2+26" orange alert

311   periods, NO_3^- became the dominant $PM_{2.5}$ components. Except for the pollution episode in March

312   2018, the proportion of another major ion NH_4^+ was generally consistent during the four pollution

313   episodes. The mean mass concentrations and proportions of SO_4^{2-}, NO_3^-, and NH_4^+ during the four

314   pollution episodes are shown in Table 4.

315   **Table 4. The mean mass concentration and percent of three major $PM_{2.5}$ components during**

316   **four pollution episodes**

Pollution Episode	SO_4^{2-}		NO_3^-		NH_4^+	
	Concentration ($\mu g/m^3$)	Percent	Concentration ($\mu g/m^3$)	Percent	Concentration ($\mu g/m^3$)	Percentage
March, 2013 **(No emission-reduction)**	45.11	39.92%	34.63	30.65%	27.14	24.02%
March, 2018 **("2+26" strategy)**	20.24	14.66%	50.17	36.34%	14.00	10.14%
November, 2016 **(Local emission-reduction)**	14.96	30.10%	16.19	32.57%	11.66	23.45%
November, 2017 **("2+26" strategy)**	7.37	13.03%	33.42	59.06%	12.33	21.80%

317   Through comparison, we found a dramatic decrease of SO_4^{2-} and a notable increase of NO_3^-

318   during two orange alert periods. The main source for SO_4^{2-} is the combustion of fossil fuels

319   (Shimano, S. et al.,2006; Kuenen, J. et al.,2013), especially the intensive burning of sulfur coals

320   for wintertime central-heating, manufacturing and household use. The main source for NO_3^- is

321   vehicle exhaust (Rodríguez, S. et al.,2004; Watson, J. G. et al.,2007; Zeng, F. et al.,2010). NH_4^+ is

322   the secondary pollutant of urban NH_3, the main source of which is the decomposition of organic

323   elements (Frank, D. S. et al.,1980; Watson, J. G. et al.,2007) and the combustion of fossil fuels

324   (Frank, D. S. et al.,1980; Watson, J. G. et al.,2007; Pan et al., 2016). Through a novel approach,

325   Pan et al (2016) quantified that more than 90% NH_3 in the Beijing-Tianjin-Hebei Region during

326   heavy pollution episodes resulted from the combustion of fossil fuels. The large variations of

327    $PM_{2.5}$ components during these episodes was mainly attributed to long-term environmental

Atmospheric
Chemistry
and Physics
Discussions

328   policies and contingent emission-reduction measures. A large number of small polluting factories

329   in Beijing and its surrounding areas have been shut down, and the use of household coal,

330   especially coarse coal that produces large amounts of sulfate-related pollutants, has been restricted

331   significantly. In addition to long-term environmental protection policies, contingent

332   emission-reduction measures, including the temporal shut-down of many factories that consumes

333   a large amount of coal, were implemented during air pollution alert periods. Furthermore, the

334   recently launched "2+26" plan requires that areas surrounding Beijing, including many cities in

335   Hebei Province (e.g., Tangshan) well-known for their coal-based iron industries, should take

336   simultaneous emission-reduction actions during regional pollution episodes. These long-term and

337   contingent strategies led to a notable decrease of SO_4^{2-} through local emission-reduction measures

338   and a further decrease of SO_4^{2-} through "2+26" regional emission-reduction measures. Meanwhile,

339   the much lower proportion of NH_4^+ in March 2018 also indicated a sudden reduction in coal fuel

340   usage in Beijing and its neighboring areas in 2018, the major driver for which will be explained in

341   the following section. Conversely, during the four pollution episodes, no strict regulation was

342   placed on the control of vehicle exhaust. Hence, the notable decrease of SO_4^{2-} and generally

343   constant mass concentration of NO_3^- led to a rapidly rising proportion of NO_3^- among the $PM_{2.5}$

344   components during the two orange alerts.

3.3 Source apportionment during the four pollution episodes

346   Based on $PM_{2.5}$ component analysis and PSAT-based source apportionment, we further quantified

347   the relative contributions of different sources to $PM_{2.5}$ concentrations in Beijing during the four

348   pollution episodes (Fig 5). A major difference between the pollution episode in March 2013 and in

349   March 2018 was the dramatic decrease in the relative contribution of coal combustion from 40%

350   to 11%. Meanwhile, the relative contribution of vehicle exhaust increased significantly from 19%

351   to 54%, indicating that vehicle exhaust became the dominant source for the pollution episode in

352   March 2018 with the "2+26" regional emission-reduction measures. On the other hand, the

353   difference in the relative contributions of different sources between the two pollution episodes in

354   November 2016 (with local emission-reduction measures) and November 2017 (with "2+26"

355   regional emission-reduction measures) were much smaller. The major differences lied in the

356   notable increase in the relative contribution of vehicle exhaust from 29% to 40% and the decrease

357   in the relative contribution of coal combustion from 34% to 28%.

358   As described above, the continuous decrease in the relative contribution of coal combustion from

359   the pollution episodes in 2013 to the episode in 2018 resulted from the combination of long-term

Atmospheric
Chemistry
and Physics
Discussions

360 and contingent local and regional emission-reduction measures. Note that despite a similar "2+26"

361 strategy implemented, the relative contribution of coal combustion during the orange alert period

362 in November 2017 was much higher than that in March 2018. A major reason for this dramatic

363 change in a short period was the implementation of a large-scale environmental project. Before

364 November 2017, the starting point of central heating in Beijing, a regional project called "Coal to

365 Gas" had finished replacing coal-based central heating systems by gas-based systems for 1.9

366 million households in the Beijing-Tianjin-Hebei Region, leading to a 2 million-ton decrease in

367 coal consumption in the region. As a result, the relative contribution of coal combustion, which

368 was the dominant emission source for $PM_{2.5}$ in Beijing during the central-heating season from

369 November to March, decreased to a fairly low level during the orange alert period in March 2018.
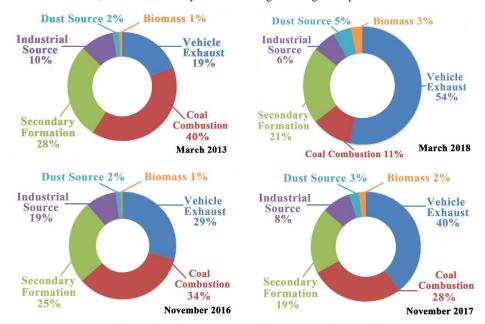

370 **Fig 5. The relative contribution of different sources to $PM_{2.5}$ concentrations in Beijing**

371 **during four pollution episodes**

372 **3.4 The relative contribution of local emission and regional transport to $PM_{2.5}$**

373 **concentrations in Beijing during the four pollution episodes**

374 Through the simulation of the WRF-CAMx model based on local and regional emission

375 inventories, we quantified the relative contributions of local emission and regional transport of

376 airborne pollutants to the variations in $PM_{2.5}$ concentrations in Beijing during four pollution

377 episodes (Fig 6). According to Fig 6, the relative contributions of local emission and regional

Atmospheric
Chemistry
and Physics
Discussions

378 transport to PM$_{2.5}$ concentrations in Beijing varied notably. For the pollution episode in March

379 2013 with no emission-reduction measures, the relative contribution of local emissions was

380 69.27%, much lower than the 88.35% for the "2+26" orange alert period in March 2018. On the

381 other hand, for the pollution episode in November 2016 with local emission-reduction measures,

382 the relative contribution of local emissions was 76.83%, much higher than the 49.46% for the

383 "2+26" orange alert period in November 2017. Meanwhile, the relative contribution to PM$_{2.5}$

384 concentrations in Beijing from specific areas also differed significantly during these pollution

385 episodes. We found that different emission-reduction strategies did not lead to a clear pattern for

386 the relative contributions of local emission and regional transport. One major reason for this is that

387 the regional transport of airborne pollutants from neighboring areas to Beijing is influenced

388 significantly by meteorological conditions, the intensity of regional emission sources and the

389 regional distribution of PM$_{2.5}$ concentrations, which demonstrated remarkable seasonal variations

390 and synoptic-scale uncertainties. From this perspective, we attempted to explain the underlying

391 drivers for the variations in local and regional contributions to PM$_{2.5}$ concentrations during the
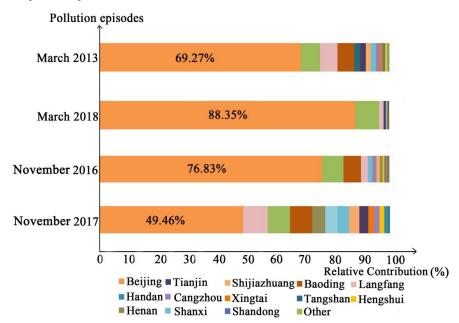
392 four pollution episodes.

393

394 **Fig 6. The relative contributions of local emission and regional transport to PM$_{2.5}$**

395 **concentrations in Beijing during the four pollution episodes**

396 For the pollution episode in March 2013, without long-term and contingent emission-reduction

397 measures, the large amount of combusted coal fuels in the neighboring areas of Beijing led to a

Atmospheric
Chemistry
and Physics
Discussions

398 relatively large regional contribution. For the pollution episode in March 2018, with the

399 implementation of the large-scale "Coal to Gas" project and "2+26" strategy, the rapidly reduced

400 coal consumption in cities surrounding Beijing and the limited restriction on the emission of local

401 vehicles led to a fairly high local contribution. For the pollution episode in November 2016, an

402 inversed temperature layer was observed with high relative humidity, which was a favorable

403 environment for the production of secondary $PM_{2.5}$ and a relatively large local contribution.

404 Despite the implementation of the "2+26" strategy, the abnormally high regional contribution for

405 the pollution episode in November 2017 could be attributed to the prevailing southerly winds that

406 brought in a large amount of air from neighboring cities (e.g., Shijiazhuang). Therefore, although

407 this pollution episode occurred in winter, it had more similarities to a summertime pollution

408 episode, which was characterized by prevailing southerly winds, thoroughly mixed pollutants

409 within the Beijing-Tianjin-Hebei Region, and notable regional transport.

4 Discussion

411 Through the comparison of the components of $PM_{2.5}$ during the pollution episode in 2013 and

412 those in 2016, 2017 and 2018, we found that the proportion of sulfate ions decreased significantly

413 while nitrite ions became the dominant component of $PM_{2.5}$ during the pollution episodes. This

414 result is consistent with findings from some recent studies (Fromme H et al., 2008; Tan J et al.,

415 2016; Shang X et al., 2018). The dramatic decrease in the proportions of SO_4^{2-} and NH_4^+ ions in

416 $PM_{2.5}$ during the pollution episode in March 2018 suggested a satisfactory effect of long-term

417 pollution control measures, especially the "Coal to Gas" project, and contingent "2+26" regional

418 emission-reduction measures on the reduction of coal combustion in the Beijing-Tianjin-Hebei

419 Region. As revealed by previous studies (Zhang R et al., 2013; Liu Y et al., 2018; Shang X et al.,

420 2018) and the source apportionment from this research, the use of coal fuels has been the

421 dominant source for the formation and mass concentration of $PM_{2.5}$ in Beijing since 2013.

422 However, the remarkable decrease in coal combustion since the winter of 2017 has greatly

423 reduced the contribution of coal combustion to local $PM_{2.5}$ concentrations, which directly

424 improved the wintertime air quality and led to the cleanest winter in Beijing since 2013. The mean

425 wintertime (the winter for Beijing here refers to the central-heating season from November 15th to

426 March 15th) $PM_{2.5}$ concentration in Beijing for 2013, 2014, 2015, 2016 and 2017 was 88.19，84.41,

427 89.39, 92.39 and 47.31 μg/ m³ respectively.

428 The implementation of the "2+26" strategy led to different effects on $PM_{2.5}$ reductions during

429   specific pollution episodes. In addition to different emission-reduction strategies, the improvement

430   of air quality in Beijing is controlled by a diversity of factors. First, meteorological conditions

431   exert a strong influence on the accumulation and dispersion of local airborne pollutants in Beijing

432   and the long-distance transport of airborne pollutants from neighboring areas. Second, the

433   distribution of $PM_{2.5}$ concentrations in the "2+26" region determines whether the air brought into

434   Beijing from neighboring areas increases or decreases $PM_{2.5}$ concentrations there. Third, the $PM_{2.5}$

435   level during pollution episodes influences the relative contributions of local and regional

436   contributions. The mean $PM_{2.5}$ concentrations during the "2+26" orange alert period in March

437   2018 was 174.24 $\mu g/m^3$. High-concentration $PM_{2.5}$ during pollution episodes led to a stagnant

438   condition with high humidity and low wind speed (Chen et al. 2017, 2018), which was an

439   unfavorable condition for the regional transport of airborne pollutants. Therefore, the relative

440   contribution of local emission to this extremely high $PM_{2.5}$ concentrations was 88.35% while the

441   relative contribution of regional transport was 11.65%. In this case, although unified

442   emission-reduction measures were implemented in its neighboring areas, the significantly

443   restricted regional transport did not fully project the effects of the "2+26" strategy to the local

444    $PM_{2.5}$ concentrations in Beijing. Conversely, the mean $PM_{2.5}$ concentrations during the "2+26"

445   orange alert period in November 2017 was 92.91 $\mu g/m^3$, which was not high enough to

446   significantly prevent the regional transport of airborne pollutants. Therefore, the "2+26" strategy

447   led to a simultaneous reduction in $PM_{2.5}$ concentrations in this region and a large amount of clean

448   air from its neighboring cities that significantly diluted the local $PM_{2.5}$ in Beijing. Consequently,

449   the relative contribution of regional transport was larger than 50% and thus the "2+26" strategy

450   achieved a much better effect on $PM_{2.5}$ reductions than that in March 2018.

451   Another dominant factor that influences the effects of the "2+26" strategy is the level of air

452   pollution alert and its corresponding emission-reduction measures. With the launch of orange air

453   pollution alerts, a series of restrictions are placed on the temporary shut down of polluting

454   factories and the emission of fossil fuels can be reduced significantly. However, during orange

455   alert periods, only the use of a small proportion of vehicles that cannot meet Environmental

456   Standards Level I and II are forbidden whilst no additional regulation is implemented on the use

457   of more than 5 million private cars in Beijing. As a result, the relative contribution of vehicle

458   exhaust increased rapidly during two of the "2+26" orange alert periods. Especially for the orange

459   alert period in March 2018, vehicle exhaust contributed to more than 50% of the high $PM_{2.5}$

460   concentrations that were higher than 174.24 $\mu g/m^3$. With dramatically reduced use of coal fuels in

461 the Beijing-Tianjin-Hebei Region due to the recent completion of the "Coal to Gas" project, the

462 control of vehicle exhaust is increasingly crucial for managing $PM_{2.5}$ concentrations during

463 pollution episodes. In this light, red air pollution alerts, which have stricter regulations on the use

464 of vehicles, should be employed with the "2+26" regional emission-reduction strategy during

465 heavy pollution episodes. For instance, during the heavy pollution episode in March 2018, if a red

466 alert instead of the orange alert was issued, the implementation of odd–even license plate policy

467 would instantly cut the daily use of private cars in Beijing by fifty percent and significantly reduce

468 the contribution of vehicle exhaust to $PM_{2.5}$ concentrations. Given the growing contribution of

469 vehicle exhaust to $PM_{2.5}$ pollutions in Beijing, in addition to the contingent regulations during

470 pollution episodes, long-term policies, including the improvement of the public transit system, the

471 enhancement of petrol quality and promotion of electric cars, should be properly implemented for

472 further reducing vehicle-exhaust induced $PM_{2.5}$ pollutions.

473 Although the regional transport network for air pollution in Beijing has been identified, this

474 research suggested that only those cities adjacent to Beijing, such as Baoding, Shijiazhuang and

475 Lang fang, made a relatively large contribution to the $PM_{2.5}$ concentrations in Beijing whilst the

476 relative contributions of some other areas within the "2+26" framework were very limited.

477 Considering the substantial social and economic loss induced by the implementation of air

478 pollution alerts, city-specific, rather than region-wide unified emission-reduction strategies,

479 should be conducted for promoting air quality in Beijing during pollution episodes. Tight

480 measures can be implemented in cities that make large contributions while lenient measures can

481 be implemented in cities that make limited contributions to $PM_{2.5}$ concentrations. To this end,

482 future studies should place more emphasis on quantifying the relative contributions from different

483 cities to local $PM_{2.5}$ concentrations in Beijing and setting city-specific emission-reduction

484 measures for each city within the "2+26" region.

5 Conclusions

486 We compared the variations in $PM_{2.5}$ concentrations in Beijing during four recent pollution

487 episodes with different emission-reduction strategies. Based on this comparison, we found that the

488 "2+26" regional emission-reduction strategy implemented in March 2018 led to a mean $PM_{2.5}$

489 concentrations of only 16.43% lower than that during the pollution episode in March 2013, when

490 no emission-reduction measure was in place. On the other hand, the same "2+26" strategy

491 implemented in November 2017 led to a mean $PM_{2.5}$ concentrations of 32.70% lower than that

Atmospheric
Chemistry
and Physics
Discussions

492   during the pollution episode in November 2016 with local emission-reduction measures. The

493   result suggested that the effects of the "2+26" regional emission-reduction measures on $PM_{2.5}$

494   reductions were influenced by meteorological conditions, regional distribution of $PM_{2.5}$

495   concentrations and local $PM_{2.5}$ level, and could differ significantly during specific pollution

496   episodes. Based on our $PM_{2.5}$ component analysis, we found that the proportion of sulfate ions

497   decreased significantly and nitrate ions were the dominant $PM_{2.5}$ components during the two

498   "2+26" orange alert periods. The source apportionment revealed that the relative contribution of

499   coal combustion to $PM_{2.5}$ concentrations during the pollution period in March 2013, November

500   2016, November 2017 and March 2018 was 40%, 34%, 28% and 11% respectively, indicating that

501   the recent completion of the large-scale "Coal to Gas" project and contingent "2+26" regional

502   emission-reduction measures led to a dramatic decrease in coal combustion in the

503   Beijing-Tianjin-Hebei Region. Meanwhile, with no specific regulation on the use of private cars,

504   the relative contribution of vehicle exhaust during the "2+26" orange alert periods in November

505   2017 and March 2018, was 40% and 54% respectively. The relative contribution of local

506   emissions to $PM_{2.5}$ concentrations in Beijing varied significantly and ranged from 49.46% to

507   89.35% during the four pollution episodes. With gradually reduced coal consumption in the

508   Beijing-Tianjin-Hebei region, this research suggested that the "2+26" regional emission-reduction

509   strategy should be implemented with red air pollution alerts to intendedly reduce the dominant

510   contribution of vehicle exhausts to $PM_{2.5}$ concentrations. Meanwhile, emission-reduction policies

511   should be designed and implemented accordingly for different cities within the "2+26" regional

512   framework. The methodology and findings from this research provided useful reference for

513   comprehensively understanding the effects of the "2+26" strategy, and for better implementation

514   of future long-term and contingent emission-reduction measures during heavy pollution episodes.

Acknowledgement

Atmospheric
Chemistry
and Physics
Discussions

Author contribution

524

525 Chen, Z., Xu, B and Yang, L. designed this research. Chen, Z wrote this manuscript. Chen, D.,

526 Zhuang, Y, Cheng, N, Gao, B. Li, R. and Zhao, B conducted data analysis. Chen, D and Zhuang, Y.

527 produced the figures. Kwan, M., Yang, L. and Chen, B helped revise this manuscript.

Atmospheric
Chemistry
and Physics
Discussions

References

1. An, X.Q., Zhu, T., Wang, Z.F., Li, C.Y., Wang, Y.S.: A modeling analysis of a heavy air pollution episode occurred in Beijing, Atmospheric Chemistry and Physics,7(12), 3103-3114, doi:10.5194/acp-7-3103-2007,2007.

2. Boylan, J. W., Russell, A. G.: PM and light extinction model performance metrics, goals, and criteria for three-dimensional air quality models, Atmospheric Environment, 40(26),4946-4959,2006.

3. Burr, M. J., Zhang, Y.: Source apportionment of fine particulate matter over the Eastern U.S. Part II: Source apportionment simulations using CAMx/PSAT and comparisons with CMAQ. source sensitivity simulations, Atmospheric Pollution Research, 2(3), 318–336,2011.

4. Chen, Z. Y., Cai, J., Gao, B. B., Xu, B., Dai, S., He, B., Xie, X. M.: Detecting the causality influence of individual meteorological factors on local $PM_{2.5}$ concentrations in the Jing-Jin-Ji region, Scientific Reports, 7, 40735,2017.

5. Chen, Z.Y., Xie, X., Cai, J., Chen, D., Gao, B., He, B., Cheng, N., Xu, B.: Understanding meteorological influences on $PM_{2.5}$ concentrations across China: a temporal and spatial perspective, Atmospheric Chemistry and Physics, 18, 5343-5358,2018.

6. Cheng, N., Zhang, D., Li, Y., Xie, X., Chen, Z., M, F., Gao, B.B., He, B.: Spatio-temporal variations of $PM_{2.5}$ concentrations and the evaluation of emission reduction measures during two red air pollution alerts in Beijing, Scientific Reports, 7(1), 8220,2017.

7. ENVIRON. User Guide for Comprehensive Air Quality Model with Extensions Version 6.0. ENVIRON International Corporation, Novato, California[EB/OL].

8. Frank D S, Ponticello I S.: Method, composition and elements for the detecting of nitrogen-containing compounds: US, US4194063, 1980.

9. Fromme, H., Diemer, J., Dietrich, S.: Chemical and morphological properties of particulate matter (PM, $PM_{2.5}$) in school classrooms and outdoor air, Atmospheric Environment, 42(27),6597-6605,2008.

10. Garrett, P., Casimiro, E.: Short-term effect of fine particulate matter ($PM_{2.5}$) and ozone on daily mortality in Lisbon, Portugal, Environmental Science and Pollution Research. 18(9), 1585-1592,2011.

11. Guaita, R., Pichiule, M., Maté, T., Linares, C., Díaz, J.: Short-term impact of particulate matter ($PM_{2.5}$) on respiratory mortality in Madrid, International Journal of Environmental Health Research, 21(4), 260-274,2011.

12. Guo, S., Hu, M., Guo, Q., Zhang, X., Zheng, M., and Zheng, J.: Primary sources and secondary formation of organic aerosols in Beijing, china, Environmental Science & Technology, 46(18), 9846-53,2012.

13. Huang, Q., Cheng, S., Perozzi, R. E.: Use of a MM5–CAMx–PSAT Modeling System to Study SO_2, Source Apportionment in the Beijing Metropolitan Region, Environmental Modeling & Assessment, 17(5):527-538,2012.

14. Kuenen, J., Gschwind B, Drebszok, K. M.: Estimating particulate matter health impact related to the combustion of different fossil fuels, Conference on Environmental Informatics - Informatics for Environmental Protection, Sustainable Development and Risk

Atmospheric
Chemistry
and Physics
Discussions

Management,171,2013.

15. Li, X., Zhang, Q., Zhang, Y.: Source contributions of urban $PM_{2.5}$ in the Beijing–Tianjin–Hebei region: Changes between 2006 and 2013 and relative impacts of emissions and meteorology, Atmospheric Environment, 123, 229-239,2015.

16. Li, Y., Ma, Z., Zheng, C., Shang, Y.: Ambient temperature enhanced acute cardiovascular-respiratory mortality effects of PM2.5 in Beijing, China, International Journal of Biometeorology, 10.1007/s00484-015-0984-z ,2015.

17. Liu Y, Yan C, Zheng M.: Source apportionment of black carbon during winter in Beijing, Science of the Total Environment, 618,531-541,2018.

18. Liu, X.H., Zhang, Y., Cheng, S.H., Xing, J., Zhang, Q., Streets, D.G., Jang, C., Wang, W.X., Hao, J.M.: Understanding of regional air pollution over China using CMAQ part I performance evaluation and seasonal variation, Atmospheric Environment,44(20), 2415-2426,2010.

19. MEP.: 2017 air pollution prevention and management plan for the Beijing-Tianjin-Hebei region and its surrounding areas,2017.

20. Pan, Y., Tian, S., Liu, D., Fang, Y., Zhu, X., & Zhang, Q.: Fossil fuel combustion-related emissions dominate atmospheric ammonia sources during severe haze episodes: evidence from 15n-stable isotope in size-resolved aerosol ammonium, Environmental Science & Technology, 50(15), 8049,2016.

21. Pascal, M., Falq, G., Wagner, V., Chatignoux, E., Corso, M., Blanchard, M., Host, S., Pascal, L., Larrieu, S.: Short-term impacts of particulate matter (PM_{10}, $PM_{10-2.5}$, $PM_{2.5}$) on mortality in nine French cities, Atmospheric Environment. 95, 175–184,2014.

22. Rodríguez, S., Querol, X., Alastuey, A.: Comparative PM10-PM2.5 source contribution study at rural, urban and industrial sites during PM episodes in Eastern Spain, Science of the Total Environment, 328(1),95-113,2004.

23. Shang, X., Lee, M., Meng, F.: Characteristics and source apportionment of fine haze aerosol in Beijing during the winter of 2013, Atmospheric Chemistry & Physics, 18(4),1-27,2018.

24. Shimano, S., Asakura, S.: The redox combustion of carbon monoxide for recovering pure carbon dioxide by using molten $(Na^+, K^+)2(CO_3^{2-}, SO_4^{2-})$ mixtures, Chemosphere, 63(10),1641,2006.

25. Tan, J., Duan, J., Zhen, N.: Chemical characteristics and source of size-fractionated atmospheric particle in haze episode in Beijing, Atmospheric Research, 167,24-33,2016.

26. Wang, X., Wei, W., Cheng, S.: Characteristics and classification of $PM_{2.5}$, pollution episodes in Beijing from 2013 to 2015, Science of the Total Environment, 612,170-179,2017.

27. Watson, J. G., Barber, P. W., Chang, M. C. O.: Southern Nevada Air Quality Study - Final Report, Diesel Engine Exhaust Gases, 7(3),279-312,2007.

28. Wu, D., Fung, J. C. H., Yao, T.: A study of control policy in the Pearl River Delta region by using the particulate matter source apportionment method, Atmospheric Environment, 76(76),147-161,2013.

29. Xing, J., Wang, S. X., Jang, C.: Nonlinear response of ozone to precursor emission changes in China: a modeling study using response surface methodology, Atmospheric Chemistry & Physics, 11(10),5027-5044,2011.

30. Zeng, F., Shi, G. L., Li. X.: Application of a Combined Model to Study the Source Apportionment of PM_{10} in Taiyuan, China, Aerosol & Air Quality Research,

10(2):177-184,2010.

31. Zeng, W., Lang, L., Li, Y.: Estimating the Excess Mortality Risk during Two Red Alert Periods in Beijing, China, International Journal of Environmental Research & Public Health, 15(1),50,2018.

32. Zhang, R., Jing, J., Tao, J.: Chemical characterization and source apportionment of $PM_{2.5}$ in Beijing: seasonal perspective, Atmospheric Chemistry & Physics, 13(14),7053-7074,2013.

33. Zhang, Z., Gong, D., Kim, S. J.: Cause and predictability for the severe haze pollutions in downtown Beijing during November-December 2015, Science of the Total Environment, 592,2017.

34. Zhong, J., Zhang X, Wang, Y.: Relative contributions of boundary-layer meteorological factors to the explosive growth of $PM_{2.5}$, during the red-alert heavy pollution episodes in Beijing in December 2016, Journal of Meteorological Research, 31(5):809-819,2017.